ROYAL SOCIETY
OF CHEMISTRY

PAPER

Check for updates

A novel water-from-air technology: creeping clathrate desalination of deliquescent salt solutions

Anke Snauwaert, [iD] [a] Estelle Becquevort, [iD] [abc] Maarten Houlleberghs, [iD] [ab] Sambhu Radhakrishnan, [iD] [ab] Eric Breynaert [iD] [abc] and Johan Martens [iD] *[a]

Water scarcity is an escalating global challenge driven by population growth and resource depletion. Conventional fresh water production methods typically require access to liquid water sources, limiting their applicability in remote or arid regions. Water-from-air technologies offer a potential solution but are often hindered by high energy demands and/or climatological conditions. This study introduces clathrate-based desalination of deliquescent salt solutions as a novel approach for atmospheric water harvesting, with potassium acetate selected as the model salt. Potassium acetate deliquesces at a relative humidity as low as 23.3%, producing a concentrated saline solution (17.8 wt% at 90% RH). By exploiting the clathrate creeping phenomenon, where hydrates grow along surfaces, enabling facilitated phase separation, 84% purification of this brine was achieved. Advanced architectures, further enhancing the crucial clathrate creeping potentially lead to further improvements of the obtained results. This process demonstrates the potential of an energy-efficient alternative to existing water-from-air technologies.

Water impact

This work introduces clathrate-based desalination of deliquescent salt solutions as a novel approach to harvest water directly from air. By avoiding the need for liquid water resources, the process offers potential for fresh water generation in off-grid areas. Utilization of the clathrate creeping phenomenon leads to strongly improved results, solving the most critical challenge for clathrate-based desalination.

Introduction

Predictions reveal that by 2030, the global demand for fresh water will exceed its supply by 40%, impacting half of the world's population.[1] As groundwater resources become increasingly depleted and the quality of accessible water deteriorates, the emphasis shifts toward the production of additional fresh water.[2,3] Conventional approaches such as wastewater purification and seawater desalination have undergone substantial improvements over recent decades, becoming nearly as efficient as is theoretically achievable.[3] However, these methods rely on the availability of liquid water sources, an assumption that does not hold in remote and/or off-grid areas. Seawater desalination techniques in

general have the additional disadvantage of producing a brine that is deposited back in the ocean, locally causing disturbance of the marine environment.[4] To address this, water-from-air technologies utilizing the ubiquitous water vapor in the atmosphere, are under development. State-of-the-art methods include active air cooling, which condenses water vapor directly from the air, and the use of desiccants, that ad/bsorb water from the atmosphere and require evaporation followed by condensation to extract the captured water in liquid form.[3,5–7] Among desiccants, deliquescent salts are of particular interest due to their ability to liquefy upon exposure to humid air, thereby enabling high water uptake values.[8,9] Fresh water is currently recovered from such salts through thermal regeneration (*i.e.* evaporation and condensation), analogous to what is done for nanoporous desiccants. However, even with the latest adsorbent material developments,[10,11] this approach remains energetically costly, primarily due to the high latent heat associated with the phase transitions of water.[3]

To reduce the energy demand of this process, Peeters *et al.*[3] proposed an alternative regeneration method for salt

[a] Centre for Surface Chemistry and Catalysis Characterisation and Application Team (COK-KAT), KU Leuven, Leuven 3001, Belgium.
E-mail: johan.martens@kuleuven.be
[b] NMRCoRe-NMR/X-Ray platform for Convergence Research, KU Leuven, Leuven 3001, Belgium
[c] Center for Molecular Water Science (CMWS), Notkestraße 85, 22607 Hamburg, Germany

2926 | *Environ. Sci.: Water Res. Technol.*, 2025, **11**, 2926–2934

This journal is © The Royal Society of Chemistry 2025

desiccants, treating the process as desalination of a saline solution rather than the regeneration of a solid desiccant. The concept, termed DESARO (DEliquescent SAlt Reverse Osmosis), uses a semi-permeable membrane to extract fresh water under applied pressure, mirroring conventional seawater reverse osmosis. The DESARO principle is promising with theoretical maximum specific water yields strongly outperforming those of the conventional water-from-air techniques. However, practical implementation remains elusive due to the operational limitations of current membrane materials. While effective for seawater (operating at 55–80 bar to overcome osmotic pressures starting around 25 bar and increasing throughout the process), the approach is not directly transferable to highly concentrated deliquescent salt solutions.[12] A similar process as what is done for seawater desalination with a comparable yield of around 50% at a relative humidity of 80%, requires a pressure of approximately 300 bar while currently existing membranes are designed to withstand a pressure of only 80 bar.[3,13]

An alternative desalination strategy that has been experimentally validated for seawater is clathrate hydrate-based desalination.[13–18] Clathrate hydrates are crystalline compounds built up from hydrogen bonded water molecules, forming cages in which guest molecules, also referred to as hydrate formers (typically low-molecular weight gases), are contained.[19] Three main clathrate structures are known (i.e. structure I, structure II and structure H) of which the formation will depend on the size and type of the guest molecule(s).[20,21] Hydrate formation typically occurs under high gas pressure and low temperature conditions, though not necessarily below the freezing point of water. Clathrate formation has been extensively studied due to its problematic occurrence in natural gas pipelines, disturbing the flow, but is now recognized for potential applications in gas storage, separation, and water purification.[13,16,18,22–30] Clathrate-based desalination is enabled by the exclusion of salts from the crystalline hydrate structure.[15,31–35] This enables selective separation of salt-free clathrate hydrate and concentrated brine. Melting of the solid clathrate fraction, realized by temperature increase and/or pressure release, theoretically yields desalinated fresh water. The influence of the presence of salts on clathrate formation has been investigated and although exceptions exist, it is generally concluded that salts exert an inhibiting effect shifting the hydrate phase equilibrium to lower temperature and higher pressure.[15,36] Kinetics of hydrate formation are also affected negatively while the process of decomposition is completed faster. The morphology of the resulting clathrates remains unaltered and the removal efficiency of an ion is better when the hydrated ion is small and has a low hydration free energy.[14]

Proof-of-concept of clathrate based seawater desalination has been reported in multiple publications.[13–18] However, known limitations include slow formation kinetics, significant refrigeration energy requirements, and, most critically, challenges associated with physical separation of

the purified clathrate phase from the remaining concentrated brine.[13,17] These issues have hindered large-scale implementation of the technique.[13,17] A standard process with a feed of 3.5 wt% salinity (standard value for seawater) realizes a desalination degree of 31%.[17] Improvement regarding this matter is accomplished by additional rinsing steps, but these cause deterioration of the yield. Pelletizing of the clathrate fraction causes purification levels up to 72–80% depending on the ions but requires pressures from 50 to 150 bar with a higher pressure resulting in better salt removal efficiency.[14,17]

This study proposes clathrate hydrate formation as a novel route to desalinate deliquescent salt solutions, offering a decentralized, low-footprint, water-from-air technology particularly suited for off-grid applications (Fig. 1). Potassium acetate (KAc) is selected as the desiccant salt due to its non-toxic nature and low deliquescence relative humidity of 22.5%, making it suitable for liquefaction at relatively dry ambient conditions.[37,38] Pressurization of the concentrated KAc solution, obtained by absorption of atmospheric water vapor, in presence of a hydrate forming gas, in this study CH_4, and lowering of the temperature initiates clathrate hydrate formation. Clathrate nucleation and growth are known to occur primarily at the water-hydrate former interface. Enhancement of this interfacial area (e.g. through stirring or gas bubbling) has a direct positive effect on hydrate formation kinetics.[39] Within a reactor, nucleation typically initiates at the reactor wall, which serves as a favourable site due to its solid surface providing a triple phase boundary. This is influenced by the contact angle at the wall, which may be modified by the presence of surfactants.[18,40,41] After nucleation at the triple phase
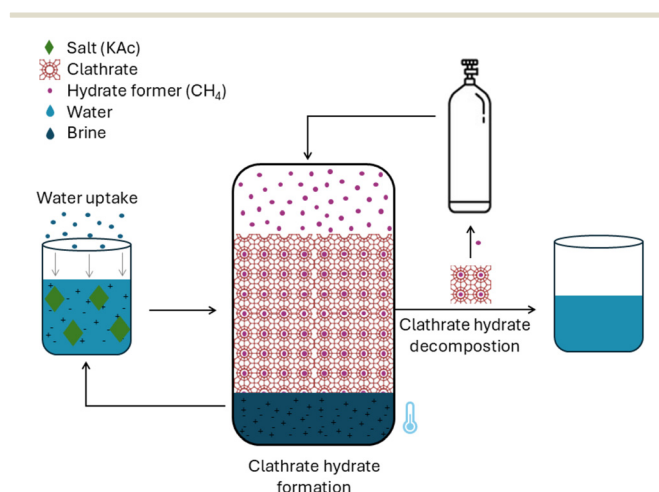

Fig. 1 Schematic of the clathrate-based deliquescent salt desalination process. The salt (e.g. KAc) liquefies upon atmospheric water uptake, forming a concentrated salt solution. Upon pressurization with a hydrate-forming gas (e.g. CH_4) and cooling, clathrate hydrates form. Physical separation of the hydrate phase from the residual brine is followed by clathrate decomposition via depressurization and temperature increase, yielding fresh water. In an ideal application, both the remaining brine and hydrate forming gas are recycled, generating a closed-loop system.

This journal is © The Royal Society of Chemistry 2025

Environ. Sci.: Water Res. Technol., 2025, **11**, 2926–2934 | **2927**

boundary, a few publications report a capillary growth process where capillary forces drive water migration from the bulk phase through interstitial voids of the hydrate mass toward the interfacial region, enabling continued clathrate growth.[40,42] This process is referred to as "clathrate creeping" due to the characteristic upward propagation of the hydrate layer along the reactor wall.[42] This paper investigates the potential of clathrate creeping to facilitate the physical separation of hydrate and brine, addressing the main bottleneck in hydrate-based seawater desalination. Finally, clathrate melting yields desalinated water and liberates the gas for reuse. In future implementations, both the hydrate former and brine could be recycled, supporting the development of a closed-loop system for atmospheric water harvesting and purification.

Experimental

Water uptake measurements

Potassium acetate (KAc, Thermo Scientific, 99+%, 150 mg) was placed in an open polypropylene recipient, and its equilibrium water uptake (g_{water}/g_{salt}) was determined at relative humidity (RH) values of 14.5, 23.3, 30.0, 40.0, 50.0, 60.0, 70.0, 80.0, and 90.0% at 25 °C. RH values between 30.0% and 90.0% were achieved using a climate chamber (Weiss Technik, Pharma 600), that was fed with deionized water. For lower RH values (14.5% and 23.3%), outside the operating range of the chamber, solutions of lithium chloride (Sigma-Aldrich, 99%) and potassium acetate (Thermo Scientific, 99+%), respectively, were employed inside a sealed desiccator including a RH-sensor (PCE-HT 114, range 0.0–100.0% (± 0.3%)). Samples were weighed daily on an analytical balance (Mettler Toledo, XSR204) until equilibrium was reached, defined as a change in mass <0.001 g between successive measurements.

NMR characterization of methane clathrate hydrate

Clathrate formation was characterized using *in situ* ^{13}C NMR spectroscopy. ^{13}C MAS NMR spectra were acquired on a 400 MHz Bruker Avance Neo spectrometer, with a 5 mm MAS probe head (Phoenix NMR) and 5 mm WHiMS high-pressure MAS rotors (Phoenix NMR).[43] A KAc solution in equilibrium with 90% RH and 25 °C was loaded in the rotor, sealed and pressurized to 70 bar with 50% ^{13}C-labeled methane (Sigma-Aldrich). The sample temperature was controlled at −15 °C using a Bruker BCU-II. Direct excitation, high power decoupling ^{13}C NMR spectra (HPDEC) were acquired under magic angle spinning at 4 kHz, using pi/2 excitation at 74 kHz, RF strength and 21.7 kHz ^{1}H decoupling using a swftppm decoupling sequence.[44] 256 transients were acquired with a recycle delay of 30 s and acquisition time of 1.024 s. Chemical shifts were externally referenced using the CH resonance of adamantane at 37.85 ppm as secondary reference.[45] Spectral decomposition of the hydrate resonances was performed using DMFit.[46]

Clathrate-based desalination experiments

Desalination tests were performed on KAc solutions obtained by deliquescence and further water absorption at 90% RH and 25 °C. Experiments were conducted in two stainless steel reactors (Fig. 2a and b). The smaller reactor (internal diameter = 1.0 cm, Fig. 2a) had a 1.90 mL chamber, that was filled with 1.00 mL solution; the total reactor volume, including pipes and the pressure gauge, was 8.26 mL. The larger reactor (internal diameter = 3.5 cm; Fig. 2b) comprised a 129 mL autoclave, yielding a total system volume of 138 mL when connected to a pressure gauge, filled with 60.0 mL of solution. Both reactors were leak-tested at 60 bar prior to experiments where no measurable pressure loss was observed over four days. In both cases, the reactor was pressurized with CH_4 to 60 bar at 22 °C, then cooled to −15 °C at a rate of ± 0.65 °C min^{-1} using an ethylene glycol refrigerated circulator (CORIO CD-200F). This set-up was again screened for leaks using a combustible gas detector (TIF8900), ensuring tightness during operation. After one hour, upon reaching the target temperature, CH_4 was added to restore the 60 bar pressure. Pressure drop during the first hour and at the end of the experiment was recorded *via* a Swagelok pressure gauge.

After two days, the reactor was depressurized to atmospheric pressure and removed from the cooling bath. The clathrate hydrate phase and residual brine were manually separated using a spatula, without washing. Clathrate decomposition occurred spontaneously upon depressurization and exposure to room temperature. Hydrate yield was calculated from the measured pressure drop according to literature, assuming a clathrate hydration number of 5.75 mol$_{water}$/mol$_{methane}$.[47] Replicates for each experiment were carried out.

Purification analysis

The aqueous phase of the decomposed clathrate hydrate was evaporated in a ventilated oven at 70 °C, and the residual salt mass was determined using an analytical balance (Mettler Toledo, XSR204). The desalination efficiency representing a
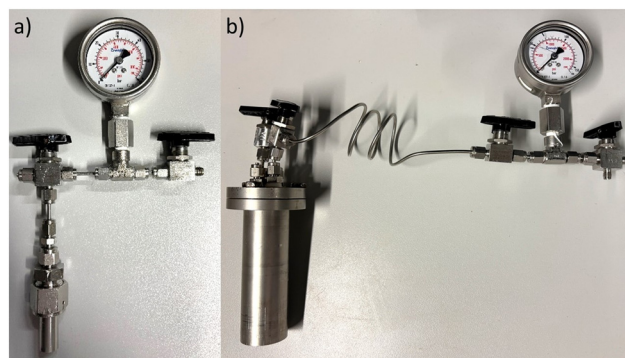

Fig. 2 Small and large stainless steel reactors (a) 8.26 mL total volume and b) 138 mL total volume for clathrate-based desalination experiments.

purification percentage was calculated relative to the initial salt concentration in the feed solution.

Results and discussion

The equilibrium water uptake of KAc as a function of relative humidity (RH) at 25 °C is shown in Fig. 3a, expressed as g_{water}/g_{KAc}. The uptake kinetics at 90% RH are presented in Fig. 3b, depicting g_{water}/g_{KAc} as a function of time. At 90% RH, the equilibrium water uptake reached 4.53 g_{water}/g_{KAc}, corresponding to a KAc solution with a salt concentration of 17.8 wt%. The static water uptake process of KAc in the climate chamber was relatively slow, with equilibrium reached only after approximately 240 h (10 days). This slow uptake rate could potentially be accelerated by enhancing convective mass transfer. Importantly, such initial uptake process starting from anhydrous KAc is only required in the first operational cycle; in subsequent cycles, the remaining brine from the clathrate desalination step is reused as the starting solution for the next water uptake (Fig. 1).

The KAc solution in equilibrium with 25 °C and RH 90% (17.8 wt%) was utilized for clathrate-based desalination experiments. To illustrate clathrate hydrate formation in this solution at the conditions used in this study, ^{13}C MAS NMR measurements were carried out. An experiment at a temperature of −15 °C and 70 bar CH_4 yielded the spectrum in Fig. 4.
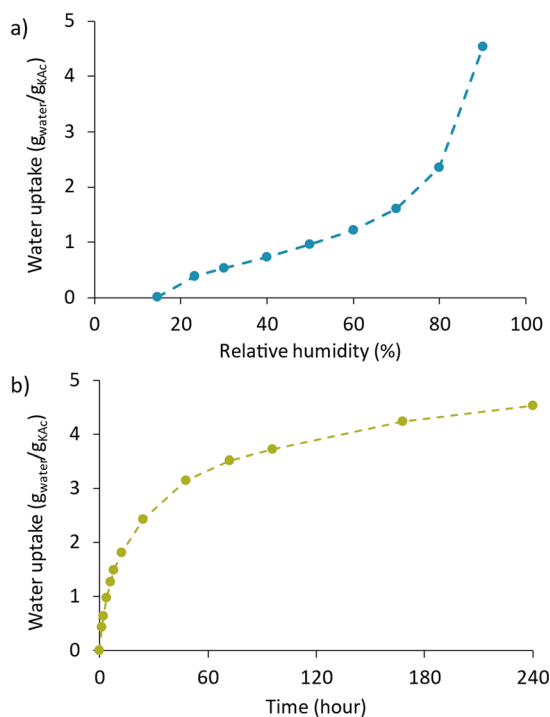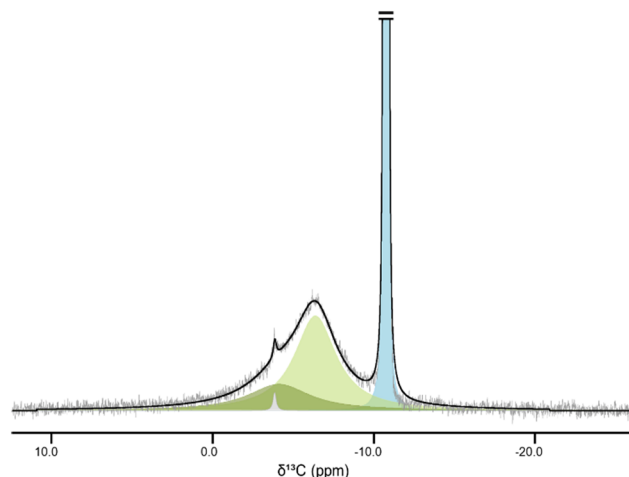

Fig. 4 ^{13}C MAS NMR spectrum of CH_4 clathrate hydrate recorded at −15 °C and 70 bar with a MAS rate of 4 kHz. The grey trace shows the measured spectrum, the black line gives the fit from spectral decomposition, which identifies four resonances: dissolved CH_4 (−3.86 ppm, light grey), CH_4 in small S^I clathrate cages (−4.13 ppm, dark green), CH_4 in large S^I clathrate cages (−6.39 ppm, light green), and free CH_4 gas (−10.76 ppm, blue).[48]

Spectral decomposition of the spectrum reveals four distinct resonances: dissolved CH_4 at −3.86 ppm (light grey), CH_4 enclathrated in small and large cages of S^I clathrate at −4.13 ppm (dark green) and −6.39 ppm (light green) respectively and free CH_4 gas at −10.76 ppm (blue).[48] This confirms successful CH_4 enclathration in both cage types of the structure I clathrate framework. Integration of the fitted peaks corresponding to CH_4 in the different cages reveals a small-to-large cage ratio of 1.2/3, reasonably close to the theoretical ratio of 1/3 for structure I clathrates. The slight deviation may be attributed to inclusion of minor amounts of acetate in the clathrate structures.

Clathrate-based desalination experiments were conducted using the small reactor (1.90 mL working volume; 8.26 mL total volume), which was filled to approximately half its working volume (1.00 mL solution). This partial filling was intended to potentially enhance the occurrence of the creeping effect.[42] The reactor, after pressurization and cooling, was maintained under clathrate-forming pressure and temperature for 48 h. Based on the observed pressure drop, the clathrate hydrate yield was estimated to contain *ca.* 35% of the water initially present for both replicates of this experiment. The characteristic "clathrate creeping" phenomenon was clearly observed, with clathrate hydrate growth extending along the reactor wall (Fig. 5a). This facilitated an efficient physical separation (Fig. 5b) of the clathrate hydrate from the residual brine, which remained at the bottom of the reactor. Subsequent decomposition of the clathrate hydrate, followed by evaporation of the recovered water, yielded an average purification degree of 81.8% (80.9% and 82.7% for the two replicates), corresponding to a KAc concentration in the recovered water of 3.1 wt%.
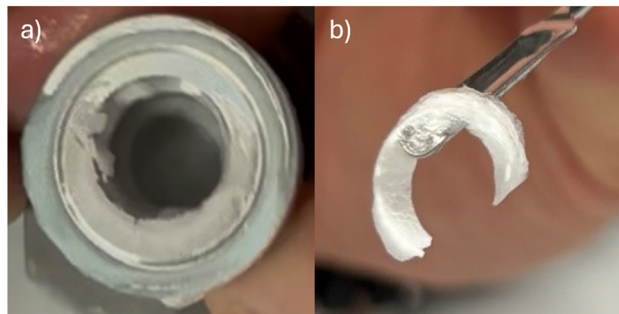

Fig. 3 a) Equilibrium water uptake (g_{water}/g_{salt}) of KAc in function of relative humidity (%) at a temperature of 25 °C. b) Time progress of water uptake (g_{water}/g_{salt}) of KAc at a relative humidity of 90% and a temperature of 25 °C.

This journal is © The Royal Society of Chemistry 2025

Environ. Sci.: Water Res. Technol., 2025, **11**, 2926–2934 | **2929**

Fig. 5 Clathrate-based desalination experiment with a 17.8 wt% solution KAc at 60 bar CH_4 and −15 °C. a) Inside of the reactor with clathrate creeping phenomenon visible at reactor wall. b) Clathrate hydrate separated from brine, facilitated by the creeping phenomenon.

Scale-up was attempted using the larger reactor (129 mL working volume; 138 mL total volume), filled approximately halfway (60 mL). After 48 h under clathrate-forming conditions, clathrate hydrate formation was observed; however, the creeping effect did not occur. Instead, the clathrate phase floated atop the brine, which significantly hindered physical separation and increased the risk of contamination with brine (Fig. S1, SI). The calculated clathrate yield, based on the pressure drop, was 10% for both replicates, and analysis of the decomposed clathrate revealed an average purification level of only 5.85% (3.98% and 7.72% for the two replicates).

These results suggest that the geometrical configuration of the system plays a decisive role in determining whether clathrate creeping occurs. Clathrate creeping typically occurs at the interface between gas, liquid and reactor wall. This interface can be quantified by the circumference (C) of this boundary in each reactor. Table 1 summarizes the geometrical considerations for the small and large reactor, including C, the liquid–gas interfacial area ($S_{liquid–gas}$), the liquid volume (V), and the reactor aspect ratio (height/diameter; (h/d)).

The ratios $C/S_{liquid–gas}$, C/V and h/d differ substantially between the two setups, with the smaller reactor providing significantly higher values. The observation of clathrate creeping in the small reactor, but not in the large one could be related to the differences in geometrical configurations for both setups. To test this hypothesis, PVC tubes (Rehau) were inserted in the large reactor, creating a larger circumference of the triple-phase boundary without affecting the other parameters. The desired creeping behaviour was successfully

Table 1 Reactor configurations (C: interface of the gas, liquid and reactor wall; $S_{liquid–gas}$: liquid–gas surface area; V: overall volume of the reactor; h = height of the reactor and d: inner diameter of the reactor)

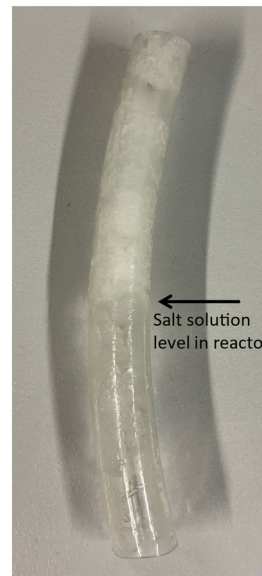| Reactor configuration	$C/S_{liquid–gas}$ (m^{-1})	C/V (m^{-2})	h/d (−)
Small reactor	400	31 415	5.80
Large reactor	114	1833.0	3.83
Large reactor with inserts	238	3822.2	

Fig. 6 Clathrate creeping in hollow PVC insert in clathrate-based desalination experiment of KAc solution (17.8 wt%). The arrow indicates the level of salt solution inside the reactor.

Salt solution level in reactor

observed inside the PVC inserts where clathrate growth extended above the bulk liquid level. The "creeping clathrate" was easily distinguished from the bulk clathrate by its whitish appearance, evidencing it's polycrystalline nature. Bulk clathrate in contrast appeared more transparent (Fig. 6). An experiment with three PVC tubes (inner diameter = 0.9 cm) yielded a water recovery of 17% for both replicates of the experiment, a clear improvement compared to experiments without inserts. The recovered creeping clathrate hydrate achieved an average purification degree of 84% with values for all three tubes in both replicate experiments ranging from 74.1% to 94.8%, *versus* a purification degree of 10–20% in the clathrate formed in the KAc solution. Following melting, the creeping clathrate and the bulk clathrate yielded aqueous solutions containing 2.85 wt% and 15.2 wt% KAc respectively. This dramatically different salt content, combined with the polycrystalline nature of the clathrate forming above the water level hints at a potential mechanism enabling the lower salt content of the creeping clathrate. Once a polycrystalline column of clathrate is established above the water level, capillary rise of water between the crystals enables water transport to the surface of the already formed clathrate. Since capillary rise has been shown to enable water deionisation,[49] the lower salt content of the creeping clathrate should no longer be surprising.

The above discussion emphasizes geometry, particularly the availability of sufficient triple-phase boundary, as a key driver of creeping. However, the contact angle between the solution and the reactor wall also plays a significant role. A contact angle below 90° is generally considered necessary for creeping to occur, with smaller values further promoting nucleation and wall growth.[40] Importantly, it has been reported that the contact angle of water on hydrophilic

surfaces increases when salts are dissolved, which may further hinder creeping in concentrated brines.[50] Both the small and large reactors were constructed from stainless steel, but differences in surface roughness likely account for variations in contact angle, which at low temperatures can range between 78° and 94°.[51,52] Such non-identical finishing may therefore contribute to the divergent behaviour observed. PVC inserts, with typically lower contact angles of around 74°,[53] consistently promoted creeping, further supporting the importance of wettability in this phenomenon.

Following creeping clathrate desalination, subsequent reverse osmosis or a combination of an additional clathrate-based desalination step (purification 90%) followed by reverse osmosis, which has been found to be an optimal system,[54] could yield fresh water that complies with drinking water standards. It should be emphasized that in real-world applications, a more comprehensive assessment of the harvested water quality is required. In addition to salinity reduction, standard water analysis methods such as total dissolved solids (TDS) measurements, ion chromatography, and microbiological testing should be employed to ensure compliance with safety and regulatory standards.

From an energy perspective, the process would greatly benefit from lower pressure requirements. To this end, difluoromethane (R-32) was evaluated as an alternative hydrate former, enabling hydrate formation at a pressure of only 8 bar while maintaining the same temperature profile as in previous experiments. A rapid pressure drop was observed, suggesting accelerated hydrate formation kinetics. However, bulk clathrate formation instead of clathrate creeping was observed and little to no purification was realized. This outcome is likely due to the high formation rate producing structural defects within the hydrate lattice, thereby impairing the exclusion of salts from the clathrate phase.

These findings indicate that slow clathrate formation kinetics are crucial to achieving high purification, as they favor the development of well-ordered hydrate structures and enable the clathrate creeping phenomenon. Creeping appears to be the primary driver of efficient salt exclusion, as it allows the clathrate phase to grow away from the bulk brine, enabling clean physical separation. The results with PVC inserts further demonstrate that targeted reactor design and the inclusion of structured surfaces or hollow tubes can significantly enhance creeping, leading to higher water yields. Optimizing geometry, surface properties, and positioning of inserts is therefore a promising route to improve process efficiency. Such design improvements are expected not only to increase yields but also to enable operation under milder pressure and temperature conditions, thereby reducing the overall energy demand.

To evaluate the energy perspective of the current process, a rough estimation of energy consumption was carried out, including CH_4 pressurization to 60 bar, cooling of the KAc solution, and the enthalpy of hydrate formation.[55] Combined with a subsequent reverse osmosis step for final purification to drinking water standards, the process yields a specific water production of 1–10 L kWh^{-1}. This already surpasses conventional desiccant-based water-from-air technologies (0.1–1 L kWh^{-1}) and is comparable to active air cooling systems (1–10 L kWh^{-1}) reported by Peeters et al.[3] While higher specific yields have been theoretically predicted for emerging water-from-air concepts (e.g. DESARO), these remain unrealized experimentally. Importantly, further optimization of creeping and reactor architecture could shift the operating window to milder hydration conditions, further lowering energy consumption and making clathrate-based desalination a competitive alternative in the field of water-from-air technologies.

Conclusions

Creeping clathrate deliquescent salt desalination is a promising water-from-air production technique, especially for remote locations, deprived from liquid water resources. The clathrate creeping phenomenon was found to be the principle mechanism behind effective salt exclusion due to facilitated physical separation of clathrate and brine, generally reported to be the main difficulty in clathrate-based seawater desalination. Slow clathrate hydrate formation kinetics proved to be essential for achieving high water quality. Gradual growth promotes the formation of well-ordered clathrate hydrate structures, successfully excluding salt. Creeping experiments with PVC hollow tube inserts realized a water yield of 17% and a purification level of 84% from a brine with 17.8 wt% KAc. By optimizing reactor geometry and the arrangement of internal structures, it is likely that water yields can be increased substantially. Such improvements could also enable operation under much milder pressure and temperature conditions, thereby significantly improving the energy efficiency of the process, needed to compete with existing water-from-air techniques. In this way, a carefully engineered system that combines controlled hydrate growth kinetics with optimized reactor design offers strong potential for scalable and energy-efficient clathrate-based desalination.

Author contributions

Investigation: A. S. and M. H.; formal analysis: A. S. and M. H.; writing – original draft: A. S.; validation and visualization: A. S., E. Be. and S. R.; supervision: E. Br. and J. M.; conceptualization: A. S., M. H., E. Br. and J. M.; funding acquisition: E. Br. and J. M.; review and editing: S. R., E. Br. and J. M.

Conflicts of interest

There are no conflicts to declare.

This journal is © The Royal Society of Chemistry 2025

Environ. Sci.: Water Res. Technol., 2025, 11, 2926–2934 | 2931

Data availability

Data for this article are available at Harvard Dataverse at https://dataverse.harvard.edu/dataverse/CBDDSS.

This dataverse contains

- The isotherms (25 °C) for equilibrium water uptake of KAc and kinetics of water uptake at RH 90%, used for Fig. 3.
- The raw NMR data of the spectrum in Fig. 4.
- Calculations on clathrate hydrate yields based on pressure drop measurement mentioned in the results and discussion.

Supplementary information (SI) is available. See DOI: https://doi.org/10.1039/d5ew00838g.

Acknowledgements

References

1 C. Monantho-Owen and C. Brady, *Building a water-resilient future for everyone, everywhere Examining the role of the built environment in mitigating the global water crisis*, 2023.

2 International Energy Agency - IEA, World Energy Outlook 2016 - Excerpt - Water-Energy Nexus, 2016.

3 R. Peeters, H. Vanderschaeghe, J. Rongé and J. A. Martens, Fresh water production from atmospheric air: Technology and innovation outlook, *iScience*, 2021, **24**, 103266.

4 T. M. Missimer and R. G. Maliva, Environmental issues in seawater reverse osmosis desalination: Intakes and outfalls, *Desalination*, 2018, **434**, 198–215.

5 R. Peeters, H. Vanderschaeghe, J. Rongé and J. A. Martens, Energy performance and climate dependency of technologies for fresh water production from atmospheric water vapour, *Environ. Sci.: Water Res. Technol.*, 2020, **6**, 2016–2034.

6 X. Zhou, H. Lu, F. Zhao and G. Yu, Atmospheric Water Harvesting: A Review of Material and Structural Designs, *ACS Mater. Lett.*, 2020, **2**, 671–684.

7 R. Tu and Y. Hwang, Reviews of atmospheric water harvesting technologies, *Energy*, 2020, **201**, 117630.

8 L. J. Mauer and L. S. Taylor, Water-solids interactions: Deliquescence, *Annu. Rev. Food Sci. Technol.*, 2010, **1**, 41–63.

9 A. G. Tereshchenko, Deliquescence: Hygroscopicity of Water-Soluble Crystalline Solids, *J. Pharm. Sci.*, 2015, **104**, 3639–3652.

10 Z. Zheng, N. Hanikel, H. Lyu and O. M. Yaghi, Broadly Tunable Atmospheric Water Harvesting in Multivariate Metal-Organic Frameworks, *J. Am. Chem. Soc.*, 2022, **144**, 22669–22675.

11 H. Kim, S. R. Rao, E. A. Kapustin, L. Zhao, S. Yang, O. M. Yaghi and E. N. Wang, Adsorption-based atmospheric water harvesting device for arid climates, *Nat. Commun.*, 2018, **9**, 1191.

12 L. F. Greenlee, D. F. Lawler, B. D. Freeman, B. Marrot and P. Moulin, Reverse osmosis desalination: Water sources, technology and today's challenges, *Water Res.*, 2009, **43**, 2317–2348.

13 P. Babu, A. Nambiar, T. He, I. A. Karimi, J. D. Lee, P. Englezos and P. Linga, A Review of Clathrate Hydrate Based Desalination to Strengthen Energy-Water Nexus, *ACS Sustainable Chem. Eng.*, 2018, **6**, 8093–8107.

14 K. C. Kang, P. Linga, K. nam Park, S. J. Choi and J. D. Lee, Seawater desalination by gas hydrate process and removal characteristics of dissolved ions (Na+, K+, Mg2+, Ca2+, B3+, Cl-, SO42-), *Desalination*, 2014, **353**, 84–90.

15 A. Kumar, A. V. Palodkar, R. Gautam, N. Choudhary, H. P. Veluswamy and S. Kumar, Role of salinity in clathrate hydrate based processes, *J. Nat. Gas Sci. Eng.*, 2022, **108**, 104811.

16 J. Javanmardi and M. Moshfeghian, Energy consumption and economic evaluation of water desalination by hydrate phenomenon, *Appl. Therm. Eng.*, 2003, **23**, 845–857.

17 K. Park, S. Y. Hong, J. W. Lee, K. C. Kang, Y. C. Lee, M.-G. Ha and J. D. Lee, A new apparatus for seawater desalination by gas hydrate process and removal characteristics of dissolved minerals (Na+, Mg2+, Ca2+, K+, B3+), *Desalination*, 2011, **274**, 91–96.

18 P. Sahu, Clathrate hydrate technology for water reclamation: Present status and future prospects, *J. Water Process Eng.*, 2021, **41**, 102058.

19 M. Baitinger, B. Böhme, A. Ormeci and Y. Grin, in *The Physics and Chemistry of Inorganic Clathrates*, 2014, pp. 35–64.

20 L. Borchardt, M. E. Casco and J. Silvestre-Albero, Methane Hydrate in Confined Spaces: An Alternative Storage System, *ChemPhysChem*, 2018, **19**, 1298–1314.

21 A. D. Schulz and M. Zabel, *Marine Geochemistry*, 2nd edn, 2005.

22 R. G. Ciocarlan, J. Farrando-Perez, D. Arenas-Esteban, M. Houlleberghs, L. L. Daemen, Y. Cheng, A. J. Ramirez-Cuesta, E. Breynaert, J. Martens, S. Bals, J. Silvestre-Albero and P. Cool, Tuneable mesoporous silica material for hydrogen storage application via nano-confined clathrate hydrate construction, *Nat. Commun.*, 2024, **15**, 8697.

23 E. J. Beckwée, G. Watson, M. Houlleberghs, D. Arenas Esteban, S. Bals, P. Van Der Voort, E. Breynaert, J. Martens, G. V. Baron and J. F. M. Denayer, Enabling hydrate-based methane storage under mild operating conditions by periodic mesoporous organosilica nanotubes, *Heliyon*, 2023, **9**, e17662.

24 P. G. M. Mileo, S. M. J. Rogge, M. Houlleberghs, E. Breynaert, J. A. Martens and V. Van Speybroeck, Interfacial study of clathrates confined in reversed silica pores, *J. Mater. Chem. A*, 2021, **9**, 21835–21844.

25 E. J. Beckwée, M. Houlleberghs, R. G. Ciocarlan, C. V. Chandran, S. Radhakrishnan, L. Hanssens, P. Cool, J. Martens, E. Breynaert, G. V. Baron and J. F. M. Denayer, Structure I methane hydrate confined in C8-grafted SBA-15: A highly efficient storage system enabling ultrafast methane loading and unloading, *Appl. Energy*, 2024, **353**, 122120.

26 N. B. Kummamuru, R. G. Ciocarlan, M. Houlleberghs, J. Martens, E. Breynaert, S. W. Verbruggen, P. Cool and P. Perreault, Surface modification of mesostructured cellular foam to enhance hydrogen storage in binary THF/H2 clathrate hydrate, *Sustainable Energy Fuels*, 2024, **8**, 2824–2838.

27 L. Hanssens, M. Houlleberghs, C. V. Chandran, G. Watson, S. Radhakrishnan, P. Van Der Voort, J. F. M. Denayer, C. E. A. Kirschhock, J. A. Martens and E. Breynaert, Enabling low-cost decentralized power reserves adopting carbon dioxide for green methane exchange in stabilized clathrate adsorbent, *J. Energy Chem.*, 2024, **97**, 438–443.

28 H. P. Veluswamy, A. Kumar, Y. Seo, J. D. Lee and P. Linga, A review of solidified natural gas (SNG) technology for gas storage via clathrate hydrates, *Appl. Energy*, 2018, **216**, 262–285.

29 A. Kumar, H. P. Veluswamy, R. Kumar and P. Linga, Direct use of seawater for rapid methane storage via clathrate (sII) hydrates, *Appl. Energy*, 2019, **235**, 21–30.

30 M. R. Dakkumalla, P. Babu and N. Daraboina, Clathrate Hydrate Desalination Technology: A Review of Recent Progress and Future Perspectives, *Energy Fuels*, 2025, **39**, 9762–9785.

31 D. Shin, J. W. Lee, Y. Woo, M. Cha, Y. Lee, S. A. Chae, S. H. Kim, O. H. Han and J. H. Yoon, Role of Salts in Phase Transformation of Clathrate Hydrates under Brine Environments, *ACS Sustainable Chem. Eng.*, 2018, **6**, 5003–5010.

32 P. Englezos, Clathrate Hydrates, *Ind. Eng. Chem. Res.*, 1993, **32**, 1251–1274.

33 Y. Woo, C. Lee, J. H. Jeong, D. Kim, J. W. Lee, Y. Yamamoto, J. Park, M. Cha and J. H. Yoon, Clathrate hydrate formation in NaCl and MgCl2 brines at low pressure conditions, *Sep. Purif. Technol.*, 2019, **209**, 56–64.

34 M. Y. Zolotov, An oceanic composition on early and today's Enceladus, *Geophys. Res. Lett.*, 2007, **34**, 23203.

35 H. Tanaka, T. Yagasaki and M. Matsumoto, On the occurrence of clathrate hydrates in extreme conditions: Dissociation pressures and occupancies at cryogenic temperatures with application to planetary systems, *Planet. Sci. J.*, 2020, **1**, 80.

36 G. D. Holder, S. P. Zetts and N. Pradhan, Phase Behavior in Systems Containing Clathrate Hydrates; A Review, *Rev. Chem. Eng.*, 1988, **5**, 1–4.

37 C. Peng, L. Chen and M. Tang, A database for deliquescence and efflorescence relative humidities of compounds with atmospheric relevance, *Fundam. Res.*, 2022, **2**, 578–587.

38 L. Greenspan, Humidity Fixed Points of Binary Saturated Aqueous Solutions, *J. Res. Natl. Bur. Stand. A Phys. Chem.*, 1977, **81**, 89–96.

39 S. D. Seo, S. Y. Hong, A. K. Sum, K. H. Lee, J. D. Lee and B. R. Lee, Thermodynamic and kinetic analysis of gas hydrates for desalination of saturated salinity water, *Chem. Eng. J.*, 2019, **370**, 980–987.

40 A. Kumar, G. Bhattacharjee, B. D. Kulkarni and R. Kumar, Role of Surfactants in Promoting Gas Hydrate Formation, *Ind. Eng. Chem. Res.*, 2015, **54**, 12217–12232.

41 J. Yoslim, P. Linga and P. Englezos, Enhanced growth of methane-propane clathrate hydrate crystals with sodium dodecyl sulfate, sodium tetradecyl sulfate, and sodium hexadecyl sulfate surfactants, *J. Cryst. Growth*, 2010, **313**, 68–80.

42 S. K. Burla and S. R. P. Pinnelli, Enrichment of gas storage in clathrate hydrates by optimizing the molar liquid water-gas ratio, *RSC Adv.*, 2022, **12**, 2074–2082.

43 E. D. Walter, L. Qi, A. Chamas, H. S. Mehta, J. A. Sears, S. L. Scott and D. W. Hoyt, Operando MAS NMR Reaction Studies at High Temperatures and Pressures, *J. Phys. Chem. C*, 2018, **122**, 8209–8215.

44 C. Vinod Chandran, P. K. Madhu, N. D. Kurur and T. Bräuniger, Swept-frequency two-pulse phase modulation (SWf-TPPM) sequences with linear sweep profile for heteronuclear decoupling in solid-state NMR, *Magn. Reson. Chem.*, 2008, **46**, 943–947.

45 R. Hoffman, Solid-state chemical-shift referencing with adamantane, *J. Magn. Reson.*, 2022, **340**, 107231.

46 D. Massiot, F. Fayon, M. Capron, I. King, S. Le Calvé, B. Alonso, J. O. Durand, B. Bujoli, Z. Gan and G. Hoatson, Modelling one- and two-dimensional solid-state NMR spectra, *Magn. Reson. Chem.*, 2002, **40**, 70–76.

47 N. B. Kummamuru, S. W. Verbruggen, S. Lenaerts and P. Perreault, Experimental investigation of methane hydrate formation in the presence of metallic packing, *Fuel*, 2022, **323**, 124269.

48 M. Houlleberghs, S. Radhakrishnan, C. V. Chandran, A. F. Morais, J. A. Martens and E. Breynaert, Harnessing Nuclear Magnetic Resonance Spectroscopy to Decipher Structure and Dynamics of Clathrate Hydrates in Confinement: A Perspective, *Molecules*, 2024, **29**, 3369.

49 I. Trus, I. Radovenchyk, E. Halysh, E. Chuprinov, D. Benatov, H. Olena and L. Sirenko, Innovative Method for Water Deiron Ions Using Capillary Material, *J. Ecol. Eng.*, 2022, **23**, 174–182.

50 N. Sghaier, M. Prat and S. B. Nasrallah, On the influence of sodium chloride concentration on equilibrium contact angle, *Chem. Eng. J.*, 2006, **122**, 47–53.

51 J. Song, D. Zeng and L. Fan, Temperature dependence of contact angles of water on a stainless steel surface at elevated temperatures and pressures: In situ

This journal is © The Royal Society of Chemistry 2025

Environ. Sci.: Water Res. Technol., 2025, **11**, 2926–2934 | 2933

characterization and thermodynamic analysis, *J. Colloid Interface Sci.*, 2020, **561**, 870–880.

52 C. Li, J. Zhang, J. Han and B. Yao, A numerical solution to the effects of surface roughness on water–coal contact angle, *Sci. Rep.*, 2021, **11**, 459.

53 K. M. McGinty and W. J. Brittain, Hydrophilic surface modification of poly(vinyl chloride) film and tubing using physisorbed free radical grafting technique, *Polymer*, 2008, **49**, 4350–4357.

54 H. Lee, H. Ryu, J. H. Lim, J. O. Kim, J. Dong Lee and S. Kim, An optimal design approach of gas hydrate and reverse osmosis hybrid system for seawater desalination, *Desalin. Water Treat.*, 2016, **57**, 9009–9017.

55 H. Liang, Y. Duan, J. Pei and N. Wei, Study on Hydrate Phase Equilibrium Diagram of Methane Containing System Based on Thermodynamic Model, *Front. Energy Res.*, 2021, **9**, 743296.

2934 | *Environ. Sci.: Water Res. Technol.*, 2025, **11**, 2926–2934

This journal is © The Royal Society of Chemistry 2025